Correlation energy within exact-exchange adiabatic connection fluctuation-dissipation theory: Systematic development and simple approximations

Nicola Colonna,[1] Maria Hellgren,[1] and Stefano de Gironcoli[1,2]
[1]*International School for Advanced Studies (SISSA), Via Bonomea 265, I-34136 Trieste, Italy*
[2]*CRS Democritos, CNR-IOM Democritos, Via Bonomea 265, I-34136 Trieste, Italy*
(Received 27 June 2014; revised manuscript received 28 August 2014; published 26 September 2014)

We have calculated the correlation energy of the homogeneous electron gas (HEG) and the dissociation energy curves of molecules with covalent bonds from an efficient implementation of the adiabatic connection fluctuation dissipation expression including the exact-exchange (EXX) kernel. The EXX kernel is defined from first-order perturbation theory and used in the Dyson equation of time-dependent density-functional theory. Within this approximation (RPAx), the correlation energies of the HEG are significantly improved with respect to the random phase approximation (RPA) up to densities of the order of $r_s \approx 10$. However, beyond this value, the RPAx response function exhibits an unphysical divergence and the approximation breaks down. Total energies of molecules at equilibrium are also highly accurate, but we find a similar instability at stretched geometries. Staying within an exact first-order approximation to the response function, we use an alternative resummation of the higher-order terms. This slight redefinition of RPAx fixes the instability in total energy calculations without compromising the overall accuracy of the approach.

DOI: 10.1103/PhysRevB.90.125150 PACS number(s): 71.15.Mb, 71.10.Ca, 31.15.E−

I. INTRODUCTION

Kohn-Sham (KS) methods that treat exchange and correlation energy on the basis of the adiabatic connection fluctuation-dissipation (ACFD) theorem [1,2] have raised considerable interest in recent years [3–17], mainly because they provide a route to overcome the shortcomings of standard local-density-approximation/generalized-gradient-approximation density-functional theory (LDA/GGA DFT). In particular, (i) an exact expression for the exchange-correlation (xc) energy in term of the density-density response function can be derived from the ACFD theorem, providing a promising way to develop a systematic improvement for the xc functional; (ii) all ACFD methods treat the exchange energy exactly, thus canceling out the spurious self-interaction error present in Hartree energy; moreover (iii) the correlation energy is fully nonlocal and automatically includes van der Waals interactions.

The ACFD method is computationally very demanding, and most often it is limited to a post self-consistent correction where the xc energy is computed from the charge density obtained from a self-consistent calculation performed with a more traditional xc functional. The basic ingredients needed to compute the correlation energy within the ACFD formalism are the density-density response function of the noninteracting KS system and the density-density response function of a system in which the electron-electron interaction is scaled by a coupling constant. While for the former an explicit expression exists, the latter is usually calculated from the Dyson equation of time-dependent density-functional theory [18] containing the xc kernel, $f_{\rm xc}$, that needs to be approximated.

The random phase approximation (RPA) is the simplest approximation; the xc kernel is simply neglected and only the frequency-independent Coulomb or Hartree kernel is taken into account. While correctly describing van der Waals interactions [19,20] and static correlation [4,14,21], as seen, for instance, when studying H_2 dissociation, the RPA is known to overestimate the correlation energies and thus to poorly describe total energies [5,6].

In this respect, various approaches have been developed in order to correct the RPA [9,15,22]. A systematic possibility to address the shortcomings of the RPA is to include all terms up to a given power of the interaction strength in the kernel. To linear order, this implies including not only the Coulomb kernel, defining the RPA, but also an exchange contribution. The frequency-dependent exact-exchange kernel, $f_{\rm x}$, has been derived by Görling [23–25] from the time-dependent optimized effective potential (TDOEP) method and by Hellgren and von Barth [6,7,26] from a variational formulation of many-body perturbation theory (MBPT). The corresponding approximation for the density-density response function, named RPAx, is obtained by solving the Dyson equation setting $f_{\rm xc} = f_{\rm x}$ and it has been successfully used in the ACFD formula to compute correlation energies of atoms [7,13] and molecules [14,27,28].

Here we set the RPAx within the context of a general scheme that allows us to formally define a power expansion of the xc kernel combining the general ACFD theory with a many-body approach, specifically the Görling-Levy perturbation theory [29] (GLPT), along the adiabatic-connection path. To first order this reduces to the RPAx, for which an efficient implementation based on an eigenvalue decomposition of the interacting time-dependent density response function in the limit of vanishing electron-electron interaction is proposed.

In this work, the performance of the RPAx has been tested on the homogeneous electron gas (HEG) at different values of r_s as well as on the dissociation of diatomic molecules with covalent bonds, such as H_2 and N_2. The results give further support to the accuracy of the RPAx, but they also reveal an instability or pathological behavior in the low-density regime of the HEG and N_2, which leads to a breakdown of the approximation. This breakdown points to the need for including correlation or a screening of the exchange kernel. However, we show here that such a procedure is not always necessary, particularly if the aim is to calculate total energies. Instead we reduce the effect of the "bare" Coulomb interaction by omitting all higher order particle-hole and self-energy

terms. This can be achieved by expanding the RPA response function in the irreducible polarizability, approximated to first order. In this way, we are able to fix the instability and at the same time keep the overall accuracy of the RPAx.

II. SYSTEMATIC IMPROVEMENT OF THE CORRELATION ENERGY

Within the ACFD framework, a formally exact expression for the exchange-correlation energy $E_{\rm xc}$ of an electronic system can be derived [1,2]:

$$E_{\rm xc} = -\frac{1}{2}\int_0^1 d\lambda \int d\mathbf{r}\, d\mathbf{r}' \frac{e^2}{|\mathbf{r}-\mathbf{r}'|} \times \left\{ \frac{\hbar}{\pi}\int_0^\infty \chi_\lambda(\mathbf{r},\mathbf{r}';iu)\, du + \delta(\mathbf{r}-\mathbf{r}')n(\mathbf{r}) \right\}, \quad (1)$$

where $\chi_\lambda(\mathbf{r},\mathbf{r}'|iu)$ is the density-response function at imaginary frequency, iu, of a system whose electrons interact with a scaled Coulomb interaction, $\lambda e^2/|\mathbf{r}-\mathbf{r}'|$, and move in a local potential chosen in such a way to keep the electronic density fixed to the ground-state density of the fully interacting system ($\lambda = 1$). At $\lambda = 1$, the local potential is equal to the external potential (usually the nuclear potential) of the fully interacting system and $H_{\lambda=1}$ coincides with the fully interacting Hamiltonian, while at $\lambda = 0$ the local potential coincides with the KS potential and $H_{\lambda=0}$ is the KS Hamiltonian. For intermediate values of λ, the Hamiltonian of the system is [29]

$$H_\lambda = H_{\rm KS} + \lambda(W - \upsilon_{\rm H} - \upsilon_{\rm x}) - \frac{\delta E_{\rm c}^\lambda}{\delta n}, \quad (2)$$

where $\upsilon_{\rm H}$ is the Hartree potential, $\upsilon_{\rm x}$ is the local exchange potential, and $\delta E_{\rm c}^\lambda/\delta n$ is the correlation contribution to the potential. The exchange potential is defined as the functional derivative of the exact KS exchange energy,

$$E_{\rm x} = -\frac{e^2}{2}\int d\mathbf{r}\, d\mathbf{r}' \frac{\left|\sum_i^{\rm occ} \phi_i^*(\mathbf{r})\phi_i(\mathbf{r}')\right|^2}{|\mathbf{r}-\mathbf{r}'|}, \quad (3)$$

which has the same expression as the Hartree-Fock exchange energy but is evaluated with the KS orbitals $\phi_i(\mathbf{r})$. It is easy to verify that it can be derived from Eq. (1) replacing χ_λ with the noninteracting density-response function,

$$\chi_0(\mathbf{r},\mathbf{r}';iu) = \sum_{ij}(f_i - f_j)\frac{\phi_i^*(\mathbf{r})\phi_j(\mathbf{r})\phi_j^*(\mathbf{r}')\phi_i\mathbf{r}')}{\epsilon_i - \epsilon_j + i\hbar u}, \quad (4)$$

where ϵ_i, $\phi_i(\mathbf{r})$, and f_i are the KS eigenvalues, KS orbitals, and occupation numbers, respectively. Subtracting the KS exchange energy from Eq. (1), the correlation energy $E_{\rm c}$ is obtained in terms of linear density responses:

$$E_{\rm c} = -\frac{\hbar}{2\pi}\int_0^1 d\lambda \int_0^\infty du\ {\rm Tr}\{\upsilon_{\rm c}[\chi_\lambda(iu) - \chi_0(iu)]\}, \quad (5)$$

where $\upsilon_{\rm c} = e^2/|\mathbf{r}-\mathbf{r}'|$ is the Coulomb kernel and $\chi_0(iu)$ is the density-response function of the noninteracting KS system. For $\lambda > 0$, the interacting density-response function $\chi_\lambda(iu)$ can be related to the noninteracting one via a Dyson equation obtained from time-dependent density-functional theory (TDDFT):

$$\chi_\lambda(iu) = \chi_0(iu) + \chi_0(iu)\left[\lambda\upsilon_{\rm c} + f_{\rm xc}^\lambda(iu)\right]\chi_\lambda(iu), \quad (6)$$

where $f_{\rm xc}^\lambda(iu)$ is the scaled frequency-dependent xc kernel. The spatial coordinate dependence is implicit in the matrix notation. When the xc kernel is specified, one can thus determine a corresponding correlation energy via Eq. (5).

In the following, we will describe a general scheme that allows us to compute the xc kernel to a given order, thus establishing a link between the TDDFT expression for the response function in Eq. (6) and the power expansion of χ_λ in the interaction strength, which can be obtained resorting to the well-established GLPT [29] along the adiabatic-connection path.

Considering the power expansion for the xc kernel $f_{\rm xc}^\lambda = \lambda f_{\rm x} + \lambda^2 f_{\rm c}^{(2)} + \cdots$ and explicitly expanding the Dyson equation (6) in the power of the interaction strength,

$$\chi_\lambda = \chi_0 + \lambda[\chi_0(\upsilon_{\rm c} + f_{\rm x})\chi_0] + \lambda^2\left[\chi_0(\upsilon_{\rm c}+f_{\rm x})\chi_0(\upsilon_{\rm c}+f_{\rm x})\chi_0 + \chi_0 f_{\rm c}^{(2)}\chi_0\right] + \cdots, \quad (7)$$

it can be seen that the first-order kernel, $\upsilon_{\rm c} + f_{\rm x}$, is intimately related to the first-order variation of χ_λ with respect to λ, and similarly higher-order correlation contributions to the kernel are related to the corresponding power in the χ_λ expansion.

Therefore, (i) we can define an arbitrarily accurate approximation to the density-density response function considering the expansion of the kernel up to a desired order in λ:

$$\chi_\lambda^{(n)} = \chi_0 + \chi_0\left[\lambda\upsilon_{\rm c} + \lambda f_{\rm x} + \cdots + \lambda^n f_{\rm c}^{(n)}\right]\chi_\lambda^{(n)}, \quad (8)$$

where (ii) the kernel up to order λ^n can be exactly determined by comparing with the λ^n expansion of χ_λ from GLPT, and (iii) the solution of the Dyson equation for $\chi_\lambda^{(n)}$ leads to a density-density response function, which is exact to order λ^n but also contains higher-order terms.

To solve the many-body Hamiltonian in Eq. (2) so as to obtain the xc kernel to a given order in λ, the xc potential, and hence the xc energy, must be known up to the same level. This apparent circular dependence does not actually hinder the application of the procedure since, thanks to the coupling constant integration involved in Eq. (5), the knowledge of the xc energy, and therefore its functional derivatives, up to order λ^n only depends on the xc kernel up to order λ^{n-1}. Our strategy can thus be applied in a sequential way,

$$E_0 \xrightarrow{\delta/\delta n} \upsilon_{\rm KS} \xrightarrow{\rm GLPT} \chi_0 \xrightarrow{\rm ACFD} E_{\rm x} \xrightarrow{\delta/\delta n} \upsilon_{\rm x} \times \xrightarrow{\rm GLPT} \left(f_{\rm x}, \chi_\lambda^{(1)}\right) \xrightarrow{\rm ACFD} E_{\rm c}^{(r2)} \to \cdots \quad (9)$$

showing that to zeroth order, i.e., replacing χ_λ with its noninteracting counterpart χ_0, the exact-exchange KS energy is obtained; moving to the next step, the exact-exchange kernel can be derived from first-order GLPT, and we recover the so-called RPAx approximation for the response function, i.e., $\chi_\lambda^{(1)}$, and for the correlation energy, i.e., $E_{\rm c}^{(r2)}$. Notice that the RPAx correlation energy $E_{\rm c}^{(r2)}$ is exact to order λ^2 but also contains, although in an approximate way, all higher-order terms, and it should not be confused with the second perturbative correction to the correlation energy in the Görling-Levy perturbation theory [29].

The mathematical complexity of this sequential procedure increases very rapidly and makes it extremely difficult to apply already at the second order; nevertheless, the prescription is given in principle. The functional derivative of $E_{\rm c}^{(r2)}$ with

respect to the density defines the exact λ^2 correction to the Hamiltonian in Eq. (2) and allows us to apply the GLPT to second order and hence to have access to the corresponding second-order contribution to the xc kernel. Solving the Dyson equation with the improved kernel defines an approximation for the response function $\chi_\lambda^{(2)}$ which is exact up to second order. Plugging $\chi_\lambda^{(2)}$ into the ACFD formula (5) leads to an approximation for the correlation energy, $E_c^{(3r)}$, which is exact to order λ^3 but also contains, although in an approximate way, all higher-order terms.

This scheme can essentially be regarded as a revised version of the standard GLPT [24,29,30] with the additional step provided by the solution of the Dyson equation for the response function and the calculation of a nonperturbative correlation energy (all order in the coupling constant appears in $E_c^{(r2)}$ and following approximation to E_c) from the ACFD formula in Eq. (5). In this way, we expect this approach to be applicable also to small gap or metallic systems, where finite-order many-body perturbation theories break down [31,32].

Having introduce the general framework, we apply our strategy to first order in the coupling strength, hence we focus on the frequency-dependent exact-exchange kernel f_x and on the calculation of the contribution $E_c^{(r2)}$ to the correlation energy (previously denoted as RPAx [7,13] or EXXRPA [14,28]), for which we propose an efficient implementation.

III. EFFICIENT CALCULATION OF RPAx CORRELATION ENERGY

Our implementation for computing the RPAx correlation energy is based on an eigenvalue decomposition of the time-dependent response function χ_λ in the limit of vanishing coupling constant. The scheme described below is a generalization of the implementation proposed by Nguyen and de Gironcoli [8] for computing RPA correlation energies.

A. RPAx correlation energy

Let us start by defining the following generalized eigenvalue problem:

$$-\chi_0[v_c + f_x]\chi_0|\omega_\alpha\rangle = a_\alpha[-\chi_0]|\omega_\alpha\rangle, \tag{10}$$

where the eigenpairs $\{|\omega_\alpha\rangle, a_\alpha\}$ and all the operators depend implicitly on the imaginary frequency iu. Once the solution of the generalized eigenvalue problem (10) is available, the trace in Eq. (5) is simply given by

$$\mathrm{Tr}[v_c(\chi_\lambda - \chi_0)] = \sum_\alpha \left(1 - \frac{1}{1-\lambda a_\alpha}\right)\langle\omega_\alpha|\chi_0 v_c \chi_0|\omega_\alpha\rangle \tag{11}$$

and the integration over the coupling constant can be calculated analytically, leading to the final expression

$$E_c^{(r2)} = -\frac{\hbar}{2\pi}\int_0^\infty du \sum_\alpha \frac{\langle\omega_\alpha|\chi_0 v_c \chi_0|\omega_\alpha\rangle}{a_\alpha(iu)} \times \{a_\alpha(iu) + \ln[1 - a_\alpha(iu)]\}. \tag{12}$$

Notice that Eqs. (10) and (12) demonstrate that knowledge of $\chi_0 f_x \chi_0$ is sufficient for computing the RPAx correlation energy, and the exact-exchange kernel alone is not needed.

B. Exact-exchange kernel

The exact expression for $h_x = \chi_0 f_x \chi_0$ in term of the KS eigenvalues and eigenfunctions has been derived by Görling starting from the time-dependent optimized potential method equation [23] and by Hellgren and von Barth starting from the variational formulation of many-body perturbation theory [6,7]. Here we propose an alternative derivation staying within the general scheme described in the previous section.

In Sec. II, it has been shown that $h_{vx} = \chi_0(v_c + f_x)\chi_0$ is the first-order correction to the noninteracting response function χ_0 due to the switching on of the perturbation $\delta\hat{V} = \hat{W} - \hat{v}_H - \hat{v}_x$. Moreover, in the previous subsection it has been shown that the eigenvalues and eigenvectors of h_{vx} are sufficient for computing RPAx correlation energies. In what follows, we derive the exact expression for the matrix elements of h_{vx} in term of the KS eigenvalues and eigenfunctions and their first-order corrections only, and we show how they can be efficiently computed resorting to the linear-response techniques of density-functional perturbation theory [33].

Let us start by considering the matrix element of χ_0 on two arbitrary, α and β, time-dependent perturbing potentials $\Delta V = \Delta V(\mathbf{r})e^{ut}$ at imaginary frequency $\omega = iu$,

$$\chi_0^{\alpha\beta}(iu) = \langle\Delta^\alpha V|\chi_0|\Delta^\beta V\rangle = \int d^3\mathbf{r}\,\Delta^\alpha V(\mathbf{r})\Delta^\beta n(\mathbf{r};iu). \tag{13}$$

For a nondegenerate ground state, the linear-response density Δn at imaginary frequency $\omega = iu$ can be written as

$$\Delta n(\mathbf{r};iu) = \langle\Phi_0|\hat{n}(\mathbf{r})|\Delta\Phi_0^{(+)} + \Delta\Phi_0^{(-)}\rangle, \tag{14}$$

where $|\Delta\Phi_0^{\pm}\rangle$ are the first-order corrections to the KS wave function $|\Phi_0\rangle$ due to the perturbation ΔV and satisfy the linearized time-dependent KS equations,

$$[H_{KS} - (E_0 \pm i\hbar u)]|\Delta\Phi_0^{(\pm)}\rangle + \Delta V|\Phi_0\rangle = 0. \tag{15}$$

Equation (13) becomes $\chi_0^{\alpha\beta}(iu) = \langle\Phi_0|\Delta^\alpha V|\Delta^\beta\Phi_0^{(+)} + \Delta^\beta\Phi_0^{(-)}\rangle$, and if the (static) perturbation δV is turned on, the first-order correction to χ_0, i.e., h_{vx}, in the coupling constant λ can be computed:

$$h_{vx}^{\alpha\beta} = \delta\chi_0^{\alpha\beta} = \langle\delta\Phi_0|\Delta^\alpha V|\Delta^\beta\Phi_0^{(+)} + \Delta^\beta\Phi_0^{(-)}\rangle + \langle\Phi_0|\Delta^\alpha V|\delta\Delta^\beta\Phi_0^{(+)} + \delta\Delta^\beta\Phi_0^{(-)}\rangle, \tag{16}$$

where $|\delta\Delta\Phi_0\rangle$ is obtained by taking the linear variation of Eq. (15),

$$[H_{KS} - (E_0 \pm i\hbar u)]|\delta\Delta\Phi_0^{(\pm)}\rangle + [\delta V - \delta E_0]|\Delta\Phi_0^{(\pm)}\rangle + \Delta V|\delta\Phi_0\rangle = 0, \tag{17}$$

while the static correction vector $|\delta\Phi_0\rangle$ satisfies the linearized time-independent Schrödinger equation

$$[H_{KS} - E_0]|\delta\Phi_0\rangle + [\delta V - \delta E_0]|\Phi_0\rangle = 0 \tag{18}$$

with $\delta E_0 = \langle\Phi_0|\delta V|\Phi_0\rangle$.

With a simple manipulation, it is easy to show that $\delta\chi_0$ depends only on the GS wave function and its first-order corrections (and not on the second-order correction $|\delta\Delta\Phi_0\rangle$). Taking the Hermitian conjugate of Eq. (15) and

multiplying it on the right by $|\delta\Delta\Phi_0\rangle$ and Eq. (17) on the left by $\langle\Delta\Phi_0|$ and subtracting the two identities so obtained, an expression for $\langle\Phi_0|\Delta^\alpha V|\delta\Delta^\beta\Phi_0^{(-)}+\delta\Delta^\beta\Phi_0^{(+)}\rangle$ is obtained in which the second-order corrections cancel out.

The final expression for $h_{\upsilon x}^{\alpha\beta}$ becomes

$$h_{\upsilon x}^{\alpha\beta}=\langle\Delta^\alpha\Phi_0^{(-)}+\Delta^\alpha\Phi_0^{(+)}|\Delta^\beta V|\delta\Phi_0\rangle+\langle\delta\Phi_0|\Delta^\alpha V|\Delta^\beta\Phi_0^{(+)}+\Delta^\beta\Phi_0^{(-)}\rangle-[\langle\Delta^\alpha\Phi_0^{(+)}|\Delta^\beta\Phi_0^{(-)}\rangle+\langle\Delta^\alpha\Phi_0^{(-)}|\Delta^\beta\Phi_0^{(+)}\rangle]\delta E_0$$
$$+\langle\Delta^\alpha\Phi_0^{(+)}|\delta V|\Delta^\beta\Phi_0^{(-)}\rangle+\langle\Delta^\alpha\Phi_0^{(-)}|\delta V|\Delta^\beta\Phi_0^{(+)}\rangle. \quad (19)$$

Equation (19) together with Eqs. (15) and (18) define the matrix elements $h_{\upsilon x}^{\alpha\beta}$ as a function of the KS many-body ground-state wave functions $|\Phi_0\rangle$ and its first-order corrections $|\Delta\Phi_0^{\pm}\rangle$ and $|\delta\Phi_0\rangle$. Introducing their definitions in terms of the single-particle KS orbitals, ϕ_a's, and their first-order variations, $\Delta\phi_a^{(\pm)}$'s and $\delta\phi_a$'s, Eq. (19) becomes

$$\begin{aligned}h_{\upsilon x}^{\alpha\beta}=&+\sum_{ab}\langle\Delta^\alpha\phi_a^{(-)}\phi_b|W|\Delta^\beta\phi_b^{(+)}\phi_a\rangle+\sum_{ab}\langle\Delta^\alpha\phi_a^{(+)}\phi_b|W|\Delta^\beta\phi_b^{(-)}\phi_a\rangle+\sum_{ab}\langle\Delta^\alpha\phi_a^{(-)}\phi_b|W|\Delta^\beta\phi_b^{(-)}\phi_a\rangle\\&+\sum_{ab}\langle\Delta^\alpha\phi_a^{(+)}\phi_b|W|\Delta^\beta\phi_b^{(+)}\phi_a\rangle-\sum_{ab}\langle\Delta^\alpha\phi_a^{(-)}\phi_b|W|\phi_a\Delta^\beta\phi_b^{(+)}\rangle-\sum_{ab}\langle\Delta^\alpha\phi_a^{(+)}\phi_b|W|\phi_a\Delta^\beta\phi_b^{(-)}\rangle\\&-\sum_{ab}\langle\phi_b\phi_a|W|\Delta^\beta\phi_b^{(+)}\Delta^\alpha\phi_a^{(-)}\rangle-\sum_{ab}\langle\phi_b\phi_a|W|\Delta^\beta\phi_b^{(-)}\Delta^\alpha\phi_a^{(+)}\rangle+\sum_{a}\langle\Delta^\alpha\phi_a^{(-)}|V_x-v_x|\Delta^\beta\phi_a^{(+)}\rangle\\&+\sum_{a}\langle\Delta^\alpha\phi_a^{(+)}|V_x-v_x|\Delta^\beta\phi_a^{(-)}\rangle-\sum_{ab}[\langle\Delta^\alpha\phi_a^{(-)}|\Delta^\beta\phi_b^{(+)}\rangle+\langle\Delta^\alpha\phi_a^{(+)}|\Delta^\beta\phi_b^{(-)}\rangle]\langle\phi_b|V_x-v_x|\phi_a\rangle\\&+\sum_{a}\langle\delta\phi_a|\Delta^\alpha V^*|\Delta^\beta\phi_a^{(+)}+\Delta^\beta\phi_a^{(-)}\rangle+\sum_{a}\langle\Delta^\alpha\phi_a^{(+)}+\Delta^\alpha\phi_a^{(-)}|\Delta^\beta V|\delta\phi_a\rangle-\sum_{ab}\langle\delta\phi_a|\Delta^\beta\phi_b^{(+)}+\Delta^\beta\phi_b^{(-)}\rangle\langle\phi_b|\Delta^\alpha V^*|\phi_a\rangle\\&-\sum_{ab}\langle\Delta^\alpha\phi_a^{(-)}+\Delta^\alpha\phi_a^{(+)}|\delta\phi_b\rangle\langle\phi_b|\Delta^\beta V|\phi_a\rangle, \quad (20)\end{aligned}$$

where the sums run over the occupied single-particle KS state only and $|\Delta\phi_a^{(\pm)}\rangle$ and $|\delta\phi_a\rangle$ are the (conduction-band projected) variations of the occupied single-particle state. They can be efficiently computed resorting to the linear-response techniques of density-functional perturbation theory [33]:

$$\begin{aligned}&[H^0+\gamma P_\upsilon-(\varepsilon_a\pm i\hbar u)]|\Delta\phi_a^{\pm}\rangle=-(1-P_\upsilon)\Delta V|\phi_a\rangle,\\&[H^0+\gamma P_\upsilon-\varepsilon_a]|\delta\phi_a\rangle=-(1-P_\upsilon)[V_x-\upsilon_x]|\phi_a\rangle, \quad (21)\end{aligned}$$

where V_x is the nonlocal exchange operator identical to the Hartree-Fock one but constructed from KS orbitals, $P_\upsilon=\sum_a^{\rm occ}|\phi_a\rangle\langle\phi_a|$ is the projector on the occupied manifold, and γ is a positive constant larger than the valence bandwidth in order to ensure that the linear system is not singular even in the limit for $iu\to 0$.

Inserting the formal solutions for $|\Delta\phi_a^{(\pm)}\rangle$ and $|\delta\phi_a\rangle$ from Eq. (21) into Eq. (20), removing the trial perturbing potential ΔV, and sending $iu\to\omega$, the expression for $h_x(\mathbf{r},\mathbf{r}';\omega)$ previously derived in Refs. [23,28] and in Ref. [26] is recovered.

The scheme described above has been implemented in the QUANTUM ESPRESSO distribution [34]. The basic operations involved in the calculation of the matrix elements $h_{\upsilon x}^{\alpha\beta}$ are the same as those required for the calculation of the RPA energy and potential in the implementations proposed by Nguyen and de Gironcoli [8] and Nguyen *et al.* [35], respectively, meaning that our RPAx calculation has a computational cost comparable to their RPA implementations and maintains their favorable scaling.

IV. HOMOGENEOUS ELECTRON GAS

As a test for the accuracy of the RPAx approximation, we choose the simple homogeneous electron gas. The homogeneous electron gas is an idealized system of electrons moving in a uniform neutralizing background. At zero temperature it is characterized by two parameters only, i.e., the number density $n=1/(4\pi r_s^3a_B^3/3)$, or equivalently the Wigner-Seitz radius r_s, and the spin polarization $\zeta=|n^\uparrow-n^\downarrow|/(n^\uparrow+n^\downarrow)$, where $n^{\uparrow(\downarrow)}$ is the density of spin-up (-down) electrons and $n=n^\uparrow+n^\downarrow$. Despite its simplicity, (i) the HEG model represents the first approximation to metals where the valence electrons are weakly bound to the ionic cores, (ii) the system is found to display a complex phase diagram including transition to the Wigner crystal, and in addition (iii) it provides the basic ingredient of any practical density-functional calculation. The most widely used approximations for the unknown xc-energy functional are based on properties of the HEG.

A. Unpolarized HEG

We begin by studying the unpolarized HEG. While the solution of the Dyson equation is demanding in general, it becomes trivial in the case of the HEG; the response functions and the kernels are all diagonal in momentum space, and the RPAx Dyson equation can be easily solved as

$$\chi_\lambda(q,iu)=\frac{\chi_0(q,iu)}{1-\lambda[\upsilon_{\rm c}(q)+f_{\rm x}(q,iu)]\chi_0(q,iu)}, \quad (22)$$

where $\upsilon_{\rm c}(q)=4\pi e^2/q^2$ and $f_{\rm x}(q,iu)$ is the exchange kernel at a given momentum and frequency.

TABLE I. Correlation energy per particle with different kernels: RPA ($f_{xc}^{\lambda}=0$), RPAx ($f_{xc}^{\lambda}=\lambda f_x$), and quantum Monte Carlo calculation [43]. All energies are in Rydberg.

r_s	RPA	RPAx	QMC
0.5	−0.194	−0.154	−0.153
1.0	−0.157	−0.121	−0.119
3.0	−0.105	−0.077	−0.074
5.0	−0.085	−0.060	−0.056
8.0	−0.068	−0.047	−0.043
10.0	−0.061	−0.042	−0.037
11.0	−0.058		−0.035

The correlation energy per electron ϵ_c follows from Eq. (5), where the trace has been replaced by an integral over momentum q and the integration over λ has been done analytically,

$$\epsilon_c = \frac{\hbar}{2\pi^2 n}\int_0^\infty q^2 dq \int_0^\infty du\ v_c(q)\chi_0(q,iu) \times\left[1+\frac{\ln[1-K(q,iu)]}{K(q,iu)}\right]. \quad (23)$$

Here $K(q,iu)$ has been defined as

$$K(q,iu) = [v_c(q)+f_x(q,iu)]\chi_0(q,iu) = v(q)\chi_0(q,iu)+\frac{h_x(q,iu)}{\chi_0(q,iu)}. \quad (24)$$

While the Lindhard function $\chi_0(q,iu)$ at imaginary frequency iu is known exactly [32], the function $h_x(q,iu)$ can be directly derived from the general expression given in Eq. (20) and is given by a sixfold integral over crystal momenta. Its static values were computed first numerically by several authors [36–38] and later analytically by Engel and Vosko [39]. The frequency dependence of h_x has been calculated by Bronsens, Lemmens, and Devreese [40,41] for real frequencies, and by Richardson and Ashcroft [42] for imaginary frequencies. Following Bronsens *et al.*, four integrations can be done analytically using cylindrical coordinates; we used a numerical quadrature for the two remaining integrations. Our numerical integration is able to recover the analytic results of Engel and Vosko [39] in the limit $u\to 0$. Finally, the integration over momentum q and imaginary frequency u in Eq. (23) has been computed numerically. The results are listed in Table I and Fig. 1. The RPA can be easily obtained from Eqs. (23) and (24) with $h_x=0$ and can be seen to seriously overestimate the correlation energy at all densities. Including the exact exchange kernel greatly improves the basic RPA, and the RPAx correlation energy per particle is close to the accurate quantum Monte Carlo (QMC) results [43].

As expected, RPAx works well for small values of r_s and becomes less accurate when r_s increases. According to our calculation, within RPAx for $r_s > 10.6$ there is a charge-density instability with wave vector $q\approx 2k_F$. In Fig. 2, the critical behavior of the static density-density RPAx response function is shown for the full interacting system [Eq. (22), $\lambda=1$]. When the density decreases, a pronounced peak

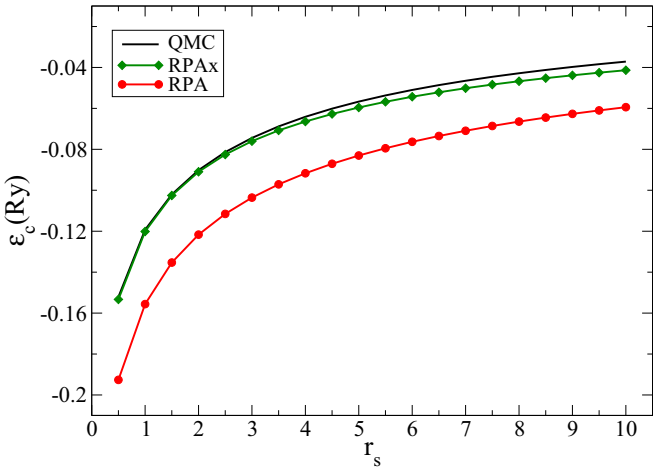

FIG. 1. (Color online) Correlation energy per particle in the homogeneous electron gas as a function of the Wigner-Seitz radius evaluated with different kernels: RPA (red squares), RPAx (green diamonds), and QMC calculation (black circles).

appears at $q\approx 2k_F$, indicating the instability with respect to charge modulations with this wave vector. As can be seen from the inset in Fig. 2, for sufficiently large values or r_s, $K=(v_c+f_x)\chi_0$ approaches unity and the denominator in Eq. (22) tends to vanish, leading to the appearance of the peak. Beyond $r_s=10.6$, K exceeds unity and the RPAx approximation breaks down as the density-density response function χ_λ is no longer negative-definite.

This instability resembles the charge-density wave instability, already observed at the Hartree-Fock level by Overhauser [32,44], and it is an artifact of the truncation of the kernel expansion to first order in the interacting strength. A full treatment of correlation in the QMC calculations moves the density instability toward the Wigner crystal to much smaller densities corresponding to $r_s\approx 80$ [43].

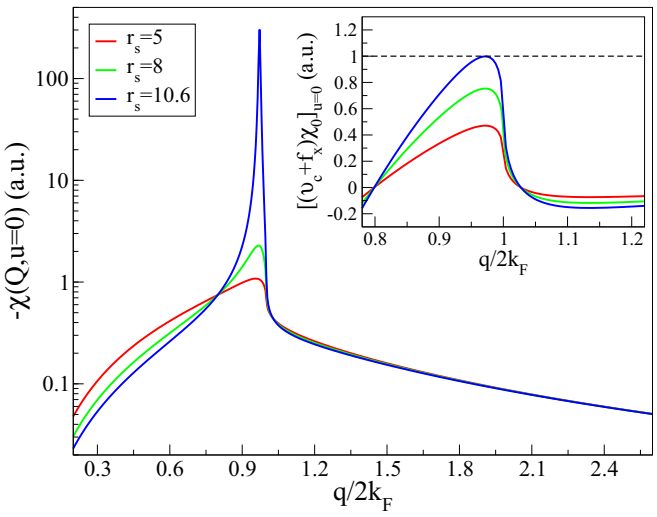

FIG. 2. (Color online) Critical behavior of the static density-density RPAx response function when the density decreases. For $r_s > 10.6$, the system becomes unstable with respect to charge modulation with wave vector $\approx 2k_F$.

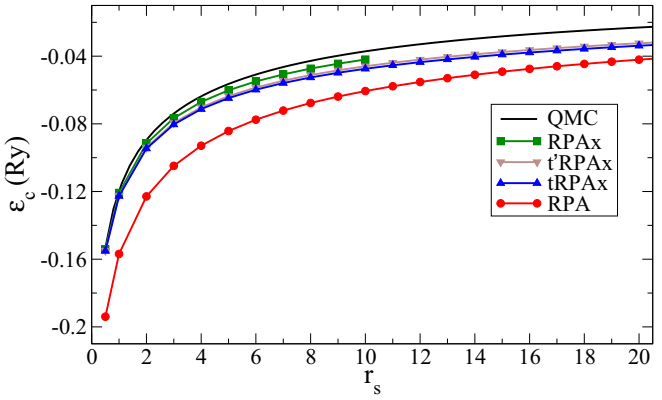

FIG. 3. (Color online) Correlation energies per particle as a function of r_s evaluated from the RPA, original and modified RPAx response functions, and compared to accurate QMC calculations.

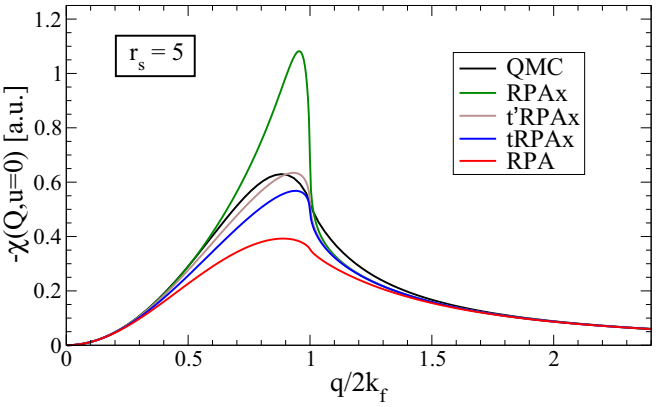

FIG. 4. (Color online) Approximate static response functions for the HEG at $r_s = 5$ as compared to the exact QMC calculations [46]. The alternative RPAx approximations show a better agreement with QMC results.

B. Alternative RPAx resummations

In Sec. II, we have established a strategy for a systematic improvement of the xc kernel. However, because of the complexity of the procedure, rather than proceeding along this way, we propose here two simple modifications to the original RPAx approximation that are able to fix the instability problem and, at the same time, to give correlation energies on the same level of accuracy as RPAx.

Introducing the irreducible polarizability P_λ, it is possible to write the interacting response function χ_λ as [39]

$$\chi_\lambda = P_\lambda + \lambda P_\lambda \upsilon_c \chi_\lambda, \tag{25}$$

where $P_\lambda = \chi_0 + \chi_0[\lambda f_x + f_c(\lambda)]P_\lambda$. Neglecting $f_c(\lambda)$ and summing up to infinite order leads again to the RPAx approximation defined above. If we instead replace P_λ with only its first-order expansion, we can define an approximation, here named tRPAx, which contains only a subset of the original RPAx expansion:

$$\chi_\lambda^{\mathrm{tRPAx}} = P_\lambda^{(1)} + \lambda P_\lambda^{(1)} \upsilon_c \chi_\lambda^{\mathrm{tRPAx}} \tag{26}$$

with $P_\lambda^{(1)} = \chi_0 + \lambda \chi_0 f_x \chi_0 = \chi_0 + \lambda h_x$. In this way, we are only including terms which contain first-order particle-hole interactions and first-order self-energy insertions.

A similar idea has been proposed in Ref. [45], where the authors suggest to expand the TDDFT response function χ_λ in a power series of the RPA response function (instead of the noninteracting one), and then to keep only the first order. This amounts to an alternative resummation, here named t′RPAx, for the interacting response function:

$$\chi_\lambda^{\mathrm{t'RPAx}} = \chi_\lambda^{\mathrm{RPA}} + \lambda \chi_\lambda^{\mathrm{RPA}} f_x \chi_\lambda^{\mathrm{RPA}}. \tag{27}$$

We notice that tRPAx and t′RPAx both only require h_x to be defined. Both approximations thus neglect all higher-order particle-hole scatterings, which in the original RPAx are simulated by the kernel.

Up to first order, the alternative RPAx response functions coincide with the original one, while they have different power expansions starting from the λ^2 term, meaning that only contributions already approximated at the RPAx level are affected by these different resummations.

Figure 3 shows the correlation energies per particle obtained starting from the alternative RPAx approximations of the response function. As expected, for high-density electron gases (small values of r_s), the correlation energies are essentially identical to the original one, since the underlying response functions are the same in the limit for $\lambda \to 0$. At the same time, they are well behaved also where the original RPAx approximation breaks down.

In Fig. 4, we compare the corresponding static density-response functions (calculated at full interaction strength $\lambda = 1$) with the exact one, obtained from QMC calculation [46], for a density corresponding to $r_s = 5$. The difference between RPA and QMC results reveals that exchange and correlation effects in the kernel are important already at this density; including the exact-exchange kernel (original RPAx) overcorrects the RPA deficiency, in particular between k_F and $2k_F$, while both of the alternative RPAx approximations are in much better agreement with accurate QMC calculations. Thus despite the fact that the RPAx energy is better at this value of r_s, the static response function is worse, suggesting that the RPAx results are subjected to a cancellation of errors when integrated over the frequency.

In the range of densities analyzed, tRPAx and t′RPAx response functions do not show any critical behavior; moreover, when the density decreases, a trend opposite to the one found for the RPAx response function is observed with a reduction (instead of the enhancement shown in Fig. 2) of the height of the peak near $2k_F$, suggesting no divergence would appear even for smaller densities.

C. Spin-polarized HEG

We continue our analysis of the HEG at the RPAx level by studying the spin-magnetization dependence of the correlation energy of the system. We start noticing that for the noninteracting system, the spin-up and spin-down components of the gas are independent, so that a simple scaling relation between the noninteracting density-density response functions of the polarized and unpolarized gas can be

derived:

$$\chi_0^{\uparrow\uparrow}[n^\uparrow] = \tfrac{1}{2}\chi_0[2n^\uparrow],$$
$$\chi_0^{\downarrow\downarrow}[n^\downarrow] = \tfrac{1}{2}\chi_0[2n^\downarrow], \qquad (28)$$

while $\chi_0^{\uparrow\downarrow} = \chi_0^{\downarrow\uparrow} = 0$.

The spin-up and spin-down components behave as independent constituents of the system at the exchange level too, and a scaling relation similar to Eq. (28) holds true also for the exchange energy [47] and, accordingly, for the exchange potential and kernel:

$$v_x^\uparrow[n^\uparrow] = v_x[2n^\uparrow], \quad f_x^{\uparrow\uparrow}[n^\uparrow] = 2f_x[2n^\uparrow],$$
$$v_x^\downarrow[n^\downarrow] = v_x[2n^\downarrow], \quad f_x^{\downarrow\downarrow}[n^\downarrow] = 2f_x[2n^\downarrow], \qquad (29)$$

while $f_x^{\uparrow\downarrow} = f_x^{\downarrow\uparrow} = 0$. Thus at the RPAx level, the interaction between the spin-up and spin-down components of the system is only mediated by the Coulomb kernel v_c.

Although more involved than for the unpolarized case, the solution of the RPAx Dyson equation for the polarized gas is nevertheless straightforward, and using the definitions in Eqs. (28) and (29), the RPAx response function of the polarized HEG can be written as

$$\chi_\lambda = \frac{\frac{1}{2}\left\{\left[\frac{\chi_0}{1-\lambda\chi_0 f_x}\right]_{2n^\uparrow} + \left[\frac{\chi_0}{1-\lambda\chi_0 f_x}\right]_{2n^\downarrow}\right\}}{1 - \frac{1}{2}\left[\frac{\lambda\chi_0 v_c}{1-\lambda\chi_0 f_x}\right]_{2n^\uparrow} - \frac{1}{2}\left[\frac{\lambda\chi_0 v_c}{1-\lambda\chi_0 f_x}\right]_{2n^\downarrow}}, \qquad (30)$$

where χ_0 and f_x are the same functions already used for the unpolarized case but evaluated at density $2n^\uparrow$ or $2n^\downarrow$.

Integrating Eq. (5) with the definition of χ_λ in Eq. (30) gives the correlation energy per particle, ϵ_c, as a function of $n^\uparrow$ and $n^\downarrow$ or, equivalently, as a function of r_s and ζ. At the RPA level, the dependence of the correlation energy on the spin magnetization was already calculated long ago by Von Barth and Hedin [51] and more recently by Vosko, Wilk, and Nusair [52]. Our RPA results, simply obtained by setting $f_x = 0$ in Eq. (30), are, within the numerical accuracy, in perfect agreement with both of the above-mentioned calculations. Figure 5 shows the spin-polarization function γ defined as

$$\gamma(r_s,\zeta) = \frac{\epsilon_c(r_s,\zeta) - \epsilon_c(r_s,0)}{\epsilon_c(r_s,1) - \epsilon_c(r_s,0)} \qquad (31)$$

for the case $r_s = 2$ evaluated at the RPA and RPAx level, and it compares it with the exchange-only dependence that is the one assumed in the Perdew-Zunger parametrization [48] of the local-spin-density approximation (LSDA) and with the Perdew-Wang parametrization [49], which is based on the more physically motivated spin-interpolation expression proposed by Vosko, Wilk, and Nusair [52]. While within RPAx the correlation energy significantly improves with respect to RPA results, there is essentially no difference between the RPA and RPAx spin-polarization functions. For this value of r_s, calculations done with the alternative resummations (tRPAx and t′RPAx) yield essentially the same results as the original RPAx and are not shown in Fig. 5. Thus for this property of the system, the RPA and all the RPAx (original and alternative) approximations give results in very good agreement with accurate quantum Monte Carlo calculations [50], performing much better than the Perdew-Zunger parametrization and slightly better than the more sophisticated Perdew-Wang parametrization.

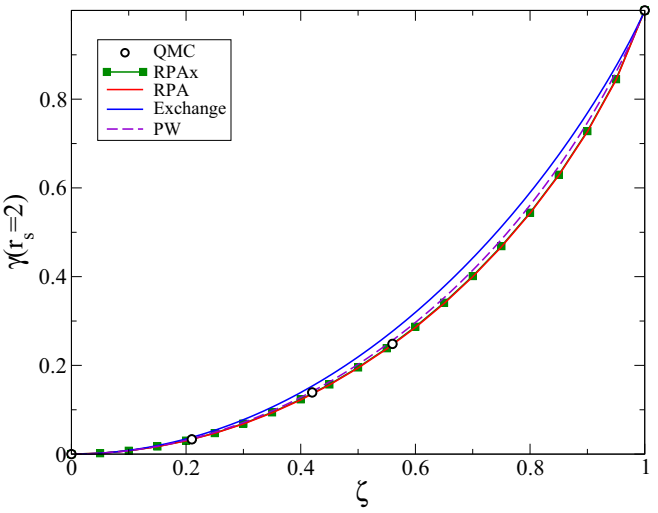

FIG. 5. (Color online) Spin-polarization function γ for $r_s = 2$ from RPA (red line), RPAX (green squares), Perdew-Zunger parametrization [48] (blue solid line), Perdew-Wang parametrization [49] (brown dashed line), and Quantum Mote Carlo calculation [50] (open circles).

V. BOND DISSOCIATION OF DIMERS

As a second test for the RPAx approximation, we studied the dissociation curve of the hydrogen and nitrogen molecules.

Within standard density-functional approximations (DFAs), the proper (singlet) KS ground state of these molecules at large interatomic separations has too high total energy (as illustrated later in Figs. 6 and 7). A better agreement with the experimental potential energy curve can be achieved resorting to a spin-polarized calculation that gives good energies, but at the expense of a qualitatively wrong spin density. In a spin-unrestricted calculation, beyond a certain value of the interatomic separation, the two spin components defining the total electron density are no longer equal, leading to a solution that is no longer a singlet, as it should be.

The H_2 and N_2 dissociation curves at the RPA level were studied previously [4,21,54]. In Refs. [4,55], the authors have shown the RPA to be size-consistent, and thus to correctly describe the dissociation without resorting to any artificial spin-symmetry breaking. However, the total energy is far too negative because of the well-known overestimation of the correlation energy [22]. Moreover, an erroneous repulsion bump appears in the dissociation curves at intermediate distances.

Recently, Heßelmann *et al.* reported the H_2 dissociation curve within the RPAx approximation, showing very good results for the total energy both around the equilibrium position R_0 and at dissociation, but still the problem of the unphysical bump at intermediate bond lengths remains. Görling and coworkers have also computed RPAx total energies for a set of 21 molecules but always in their equilibrium geometries [27,28].

Here we would like to assess the performance of the RPAx (original and alternative) approximations for molecules beyond their equilibrium geometries studying the dissociation curves of H_2 and N_2. The dimers and the corresponding isolated atoms were simulated using a simple-cubic supercell

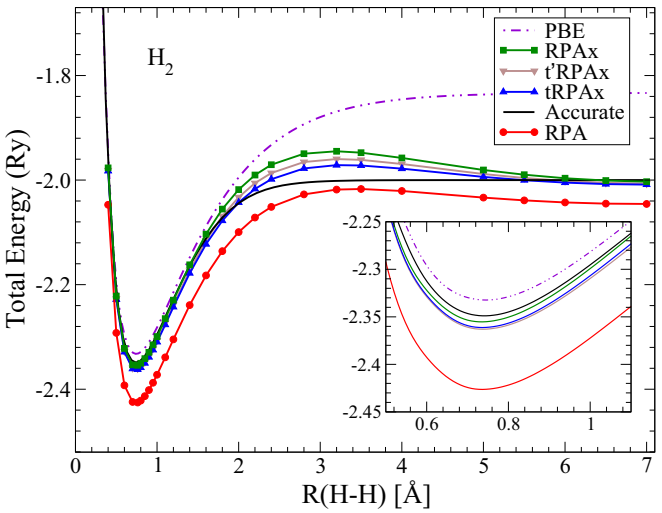

FIG. 6. (Color online) Dissociation curve of the H_2 molecule. PBE, RPA, and RPAx (original and alternative) results are compared with accurate calculations [53].

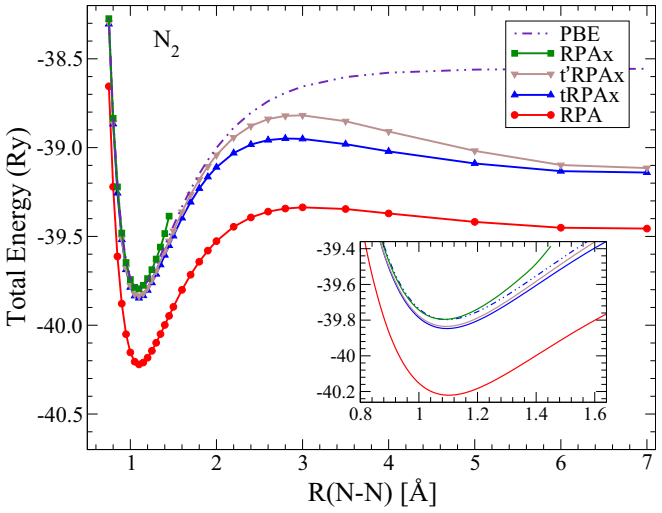

FIG. 7. (Color online) Dissociation curve of the N_2 molecule. The plot compares results from PBE, RPA, and RPAx (original and alternative) calculations.

with a size length $a = 22$ and 25 bohr, respectively. A kinetic-energy cutoff of 50 Ry was used for both systems, and up to 200 lowest-lying eigenpairs of the generalized-eigenvalue problem in Eq. (10) were used to compute the RPA and RPAx correlation energies. All the calculations have been done starting from well-converged PBE orbitals.

In Fig. 6, we report our results for the dissociation curves of H_2, and in Table II we show the structural parameters extracted from them. Comparison with accurate calculations [53] illustrates the aforementioned deficiencies of PBE and RPA dissociation curves: standard DFAs give too high total energy in the dissociation limit, while the RPA overestimates the correlation energy, leading to a curve well below the reference one. Including the exact-exchange kernel leads to a sensible improvement in the total energy description; as can be seen from the inset in Fig. 6, the RPAx total energies around the equilibrium position are in very good agreement with accurate quantum chemistry calculations. The alternative re-summations, while essentially giving the same energy as the original RPAx in the minimum region, have a positive effect on the dissociation curve at intermediate distances, reducing the height of the repulsive hump. We notice that at large interatomic separations, the RPAx approximation drops below the exact dissociation limit of 2 Ry, in agreement with the analysis reported in Ref. [4].

With the simple H_2 example in mind, we can turn to analyze the more interesting case of the N_2 molecule. In Fig. 7, we report our results for the dissociation curve, and in Table II we show the structural parameters obtained from them. As already observed for the H dimer also in this case, the whole RPA dissociation curve lies far below all the other curves. Nevertheless, the structural parameters at the RPA level are in very good agreement with results from accurate quantum chemistry calculations [56]. Including the exact-exchange contribution to the kernel corrects for the RPA overestimation of the correlation energy, shifting the RPAx dissociation curve upward. At the same time, the good performance for the equilibrium bond length and the vibrational frequency already obtained at the RPA level is maintained. However, unlike what happens for the H_2 molecule, in this case the original RPAx approximation breaks down when the nitrogen atoms are separated. For bond lengths greater than $R = 1.45$ Å, the RPAx response function is no longer negative-definite, leading to an instability that is very similar the one observed for the low-density homogeneous electron gas and, ultimately, causes the breakdown of the approximation. The alternative resummations proposed to fix the pathological behavior of the RPAx response function in the HEG turn out to be effective also in this very different situation. The tRPAx and t′RPAx dissociation curves are close to the RPAx one in the equilibrium region (see the inset in Fig. 7), but they are well-behaved also for bond lengths greater than $R = 1.45$ Å, overcoming also in this case what appears to be an intrinsic inadequacy of the original RPAx approximation.

TABLE II. Equilibrium properties of hydrogen and nitrogen dimers computed within different functionals: PBE, RPA, and all the RPAx. Accurate values extracted from dissociation curves from Ref. [53] for H_2 and from Ref. [56] for N_2 are also given. Equilibrium bond length (R_0) in Å, binding energy (E_b) in meV, and vibrational frequency (ω_0) in cm^{-1}.

	PBE	RPA	RPAx	tRPAx	t′RPAx	Refs.
H_2						
R_0 (Å)	0.755	0.740	0.738	0.742	0.738	0.741
E_b (eV)	6.78	4.85	4.41	4.48	4.45	4.75
ω_0 (cm^{-1})	4219	4520	4560	4506	4406	4529
N_2						
R_0 (Å)	1.102	1.100	1.085	1.090	1.086	1.095
E_b (eV)	16.86	9.92		9.22	9.07	9.91
ω_0 (cm^{-1})	2274	2322	2569	2430	2482	2383

VI. CONCLUSIONS

In this work, we set the RPAx approximation for the correlation energy within a general scheme that combines the general framework of the ACFD theory with a systematic many-body approach along the adiabatic-connection path, and which allow us in principle to improve the xc kernel for the purpose of calculating increasingly more accurate correlation energy. We have shown that, in a perturbative approach, the RPA is an "incomplete" approximation and that the exact-exchange kernel has to be taken into account for a consistent description to first order in the interaction strength. An efficient method for the calculation of the RPAx correlation energy has been proposed, based on an eigenvalue decomposition of the time-dependent response function of the many-body system in the limit of vanishing coupling constant.

The accuracy of the RPAx approximation has been tested on the homogeneous electron gas, revealing a great improvement over RPA results and a very good agreement with accurate QMC calculations. The spin magnetization dependency of the RPA and RPAx correlation energies has been calculated as well, showing a big improvement if compared to standard parametrization and a nearly perfect agreement with QMC calculation.

These encouraging results are, however, disturbed by the breakdown of the procedure for large values of r_s, where the RPAx density-density response function unphysically changes sign, thus indicating that correlation contributions to the kernel are needed to obtain accurate results for the HEG at low densities. Staying within an exact first-order approximation to the response function, we have suggested two simple and inexpensive modifications of the RPAx approximation that lead to a good description of the correlation energy of the system even in the limit of small densities.

We then examine molecular dissociation of H_2 and N_2 within the RPAx approximation, discovering the same virtues and vices already observed in the HEG case. A sensible improvement of the total energy description is disturbed by a pathological behavior of the response function, which ultimately poses doubts on the broad applicability of the RPAx approximation. The alternative resummations, tRPAx and t′RPAx, proposed here have been shown to be able to fix the RPAx inadequacy without compromising its virtues. Although more tests are needed in order to completely characterize them, tRPAx and t′RPAx emerge as promising and stable alternatives to the original RPAx approximation.

ACKNOWLEDGMENTS

We thank CINECA (Bologna, Italy) and SISSA (Trieste, Italy) for the availability of high performance computing resources and support.

[1] D. Langreth and J. Perdew, Solid State Commun. **17**, 1425 (1975).
[2] D. C. Langreth and J. P. Perdew, Phys. Rev. B **15**, 2884 (1977).
[3] M. Fuchs and X. Gonze, Phys. Rev. B **65**, 235109 (2002).
[4] M. Fuchs, Y.-M. Niquet, X. Gonze, and K. Burke, J. Chem. Phys. **122**, 094116 (2005).
[5] H. Jiang and E. Engel, J. Chem. Phys. **127**, 184108 (2007).
[6] M. Hellgren and U. von Barth, Phys. Rev. B **76**, 075107 (2007).
[7] M. Hellgren and U. von Barth, Phys. Rev. B **78**, 115107 (2008).
[8] H.-V. Nguyen and S. de Gironcoli, Phys. Rev. B **79**, 205114 (2009).
[9] J. Toulouse, I. C. Gerber, G. Jansen, A. Savin, and J. G. Ángyán, Phys. Rev. Lett. **102**, 096404 (2009).
[10] J. Harl and G. Kresse, Phys. Rev. Lett. **103**, 056401 (2009).
[11] J. Harl, L. Schimka, and G. Kresse, Phys. Rev. B **81**, 115126 (2010).
[12] H.-V. Nguyen and G. Galli, J. Chem. Phys. **132**, 044109 (2010).
[13] M. Hellgren and U. von Barth, J. Chem. Phys. **132**, 044101 (2010).
[14] A. Heßelmann and A. Görling, Phys. Rev. Lett. **106**, 093001 (2011).
[15] X. Ren, A. Tkatchenko, P. Rinke, and M. Scheffler, Phys. Rev. Lett. **106**, 153003 (2011).
[16] X. Ren, P. Rinke, C. Joas, and M. Scheffler, J. Mater. Sci. **47**, 7447 (2012).
[17] T. Olsen and K. S. Thygesen, Phys. Rev. Lett. **112**, 203001 (2014).
[18] E. K. U. Gross and W. Kohn, Phys. Rev. Lett. **55**, 2850 (1985).
[19] J. Dobson, *Topics in Condensed Matter Physics* (Nova, New York, 1994).
[20] E. Gross, J. Dobson, and M. Petersilka, *Density Functional Theory II (Relativistic and Time Dependent Extensions)*, edited by R. F. Nalewajski, Topics in Current Chemistry (Springer-Verlag, Berlin, 1996), Vol. 181.
[21] F. Caruso, D. R. Rohr, M. Hellgren, X. Ren, P. Rinke, A. Rubio, and M. Scheffler, Phys. Rev. Lett. **110**, 146403 (2013).
[22] S. Kurth and J. P. Perdew, Phys. Rev. B **59**, 10461 (1999).
[23] A. Görling, Int. J. Quantum Chem. **69**, 265 (1998).
[24] A. Görling, Phys. Rev. A **57**, 3433 (1998).
[25] Y.-H. Kim and A. Görling, Phys. Rev. B **66**, 035114 (2002).
[26] M. Hellgren and U. von Barth, J. Chem. Phys. **131**, 044110 (2009).
[27] A. Heßelmann and A. Görling, Mol. Phys. **108**, 359 (2010).
[28] P. Bleiziffer, A. Heßelmann, and A. Görling, J. Chem. Phys. **136**, 134102 (2012).
[29] A. Görling and M. Levy, Phys. Rev. B **47**, 13105 (1993).
[30] A. Görling, Phys. Rev. A **55**, 2630 (1997).
[31] M. Gell-Mann and K. A. Brueckner, Phys. Rev. **106**, 364 (1957).
[32] G. Giuliani and G. Vignale, *Quantum Theory of the Electron Liquid* (Cambridge University Press, Cambridge, 1971).
[33] S. Baroni, S. de Gironcoli, A. Dal Corso, and P. Giannozzi, Rev. Mod. Phys. **73**, 515 (2001).
[34] P. Giannozzi, S. Baroni, N. Bonini, M. Calandra, R. Car, C. Cavazzoni, D. Ceresoli, G. L. Chiarotti, M. Cococcioni, I. Dabo, A. D. Corso, S. de Gironcoli, S. Fabris, G. Fratesi, R. Gebauer, U. Gerstmann, C. Gougoussis, A. Kokalj, M. Lazzeri, L. Martin-Samos, N. Marzari, F. Mauri, R. Mazzarello, S.

Paolini, A. Pasquarello, L. Paulatto, C. Sbraccia, S. Scandolo, G. Sclauzero, A. P. Seitsonen, A. Smogunov, P. Umari, and R. M. Wentzcovitch, J. Phys.: Condens. Matter **21**, 395502 (2009).
[35] N. L. Nguyen, N. Colonna, and S. de Gironcoli, Phys. Rev. B **90**, 045138 (2014).
[36] D. Geldart and R. Taylor, Can. J. Phys. **48**, 155 (1970).
[37] P. R. Antoniewicz and L. Kleinman, Phys. Rev. B **31**, 6779 (1985).
[38] J. A. Chevary and S. H. Vosko, Phys. Rev. B **42**, 5320 (1990).
[39] E. Engel and S. H. Vosko, Phys. Rev. B **42**, 4940 (1990).
[40] F. Bronsens, L. Lemmens, and J. Devreese, Phys. Status Solidi B **74**, 45 (1976).
[41] F. Bronsens, L. Lemmens, and J. Devreese, Phys. Status Solidi B **80**, 99 (1977).
[42] C. F. Richardson and N. W. Ashcroft, Phys. Rev. B **50**, 8170 (1994).
[43] D. M. Ceperley and B. J. Alder, Phys. Rev. Lett. **45**, 566 (1980).
[44] A. W. Overhauser, Phys. Rev. **128**, 1437 (1962).
[45] J. E. Bates and F. Furche, J. Chem. Phys. **139**, 171103 (2013).
[46] S. Moroni, D. M. Ceperley, and G. Senatore, Phys. Rev. Lett. **75**, 689 (1995).
[47] G. L. Oliver and J. P. Perdew, Phys. Rev. A **20**, 397 (1979).
[48] J. P. Perdew and A. Zunger, Phys. Rev. B **23**, 5048 (1981).
[49] J. P. Perdew and Y. Wang, Phys. Rev. B **45**, 13244 (1992).
[50] G. Ortiz and P. Ballone, Phys. Rev. B **50**, 1391 (1994).
[51] U. von Barth and L. Hedin, J. Phys. C **5**, 1629 (1972).
[52] S. H. Vosko, L. Wilk, and M. Nusair, Can. J. Phys. **58**, 1200 (1980).
[53] W. Kolos and L. Wolniewicz, J. Chem. Phys. **43**, 2429 (1965).
[54] F. Furche, Phys. Rev. B **64**, 195120 (2001).
[55] M. Hellgren, D. R. Rohr, and E. Gross, J. Chem. Phys. **136**, 034106 (2012).
[56] R. J. Gdanitz, Chem. Phys. Lett. **283**, 253 (1998).